QUATERNARY RESEARCH 17, 135–147 (1982)

Brunhes–Matuyama Magnetic Reversal Dated at 790,000 yr B.P. by Marine–Astronomical Correlations

R. G. JOHNSON

Corporate Technology Center, Honeywell, Inc., 10701 Lyndale Avenue South, Bloomington, Minnesota 55420

Received June 9, 1980

The presence of the Brunhes–Matuyama magnetic reversal in deep-sea core sediments makes possible an alternative to the usual K/Ar radioisotope method of dating the reversal as found in rocks. The alternative method uses correlations of Northern Hemisphere summer insolation with oxygen-isotope ratios from tropical cores. The latitude-dependent insolation variations are calculated from planetary mechanics and thus provide a highly accurate astronomical time scale. The insolation variations strongly influence glacial-ice volume fluctuations that dominate the oxygen-isotope ratio changes recorded in core sediments. The summer half-year insolation variations are identified with corresponding isotope-ratio changes in cores from the present through glacial Stage 20. Misleading effects of discontinuities or major nonuniformities of sediment deposition are avoided by an analysis of the uniformity of V28-238 and V28-239, the principal cores studied, and by comparisons with other cores. The top section (Stages 1 to 10) of V28-238 is uniformly deposited, and for this section an isotope-ratio time scale is chosen that agrees with the thorium–uranium date for the high sea stand of the last interglacial extreme. Over this interval, major glacial extremes (strong isotope-ratio minima) coincide consistently with major insolation minima at times of low orbital eccentricity. In addition interstadials are directly associated with precessional insolation peaks, and the envelope of isotope-ratio peaks resembles the envelope of precessionally dominated insolation peaks. The assumption that the glacial extremes depended similarly on insolation minima during Stages 10 to 20 permits minor age shifts of strong isotope-ratio minima in the two cores (relative to ages based on uniform overall deposition) to match the ages of low-eccentricity insolation minima. The age shifts reflect residual nonuniformities of deposition. The validity of this matching procedure is supported by a resulting consistent identification of principal isotope-ratio peaks with high- and low-latitude coincident insolation maxima. The Brunhes–Matuyama reversal is found in interglacial Stage 19, and is dated on the astronomical time scale at 790,000 ± 5000 yr B.P.

INTRODUCTION

Radioisotope dating methods provide the time scale for Pleistocene events, but dates so obtained may have uncertainties due to inadequately closed isotopic decay systems and poor statistics caused by low levels of daughter products. An alternative and independent dating method applicable to the marine geological record is based on the correlation of deep-sea-core oxygen-isotope ratio ($\delta^{18}O$) variations (Emiliani, 1955) with corresponding variations in the incoming flux of Northern Hemisphere summer half-year solar radiation at the top of the atmosphere. The oxygen-isotope variations in the carbonate of planktonic foraminiferal microfossils from tropical cores are largely caused by variations in glacial ice volume (Dansgaard and Tauber, 1969). The insolation variations strongly influence glacial ice volume and are derived precisely from nearly cyclical changes in the Earth's orbital parameters. Consequently the key insolation variations are calculated on a highly accurate astronomical time scale (Berger, 1978) to which the isotope-ratio variations can be referred. This dating approach is quite applicable to the Brunhes–Matuyama magnetic reversal which is found at a prominent peak in the isotope ratios in longer cores.

The potassium–argon radioisotope method gives an age for the Brunhes boundary of 730,000 yr B.P. (Mankinen and Dal-

0033-5894/82/020135-13$02.00/0

rymple, 1979). The accuracy of this date depends on corrections for atmospheric argon contamination, the accuracy of the abundance ratios and decay constants used, and the degree of retention of the argon daughter product in the rocks from the time of solidification to the present (Cox and Dalrymple, 1967). Although the indicated precision of the reversal date may be a few tens of thousands of years corresponding to minimal variation of argon retention in rocks from widely different locations, the K/Ar date could be too young by more than this uncertainty if all rock samples near the reversal date have experienced a similar and significant argon loss.

The astronomical method offers the possibility of higher accuracy and precision on a million-year time scale and avoids the uncertainties of the K/Ar method, although in exchange, the effects of core imperfections must be recognized and corrected. In closely spaced sample intervals along the cores, the stratigraphic position of the reversal can be precisely located. Similarly, in cores with higher deposition rates, the sample intervals can define the shortest periodicity in the oxygen-isotope ratios: the often prominent 22,000-yr variation due to the orbital precession effect. The reversal can be located to within a fraction of this period. However, the precessional variations are not always prominent or clearly visible and taken alone sometimes yield ambiguous correlations over long time intervals. A more promising method used in this paper is the identification of the longer-term glacial extremes with specific intervals of low insolation.

The lack of sufficiently uniform deposition in most cores makes the reliable recognition and correlation of isotope-ratio features from core to core and between cores and insolation curves difficult over long time intervals. The two principal cores from the western tropical Pacific, V28-238 and V28-239, used in this study (Fig. 1), are perhaps unique in that, when compared, the major isotope-ratio features representing the glacial and interglacial stages can be unambiguously recognized in each core all the way to the lower Brunhes boundary. These cores are not ideally uniform, but this obstacle to the identification of isotope ratios with insolation variations is overcome by a detailed analysis of the two cores and by

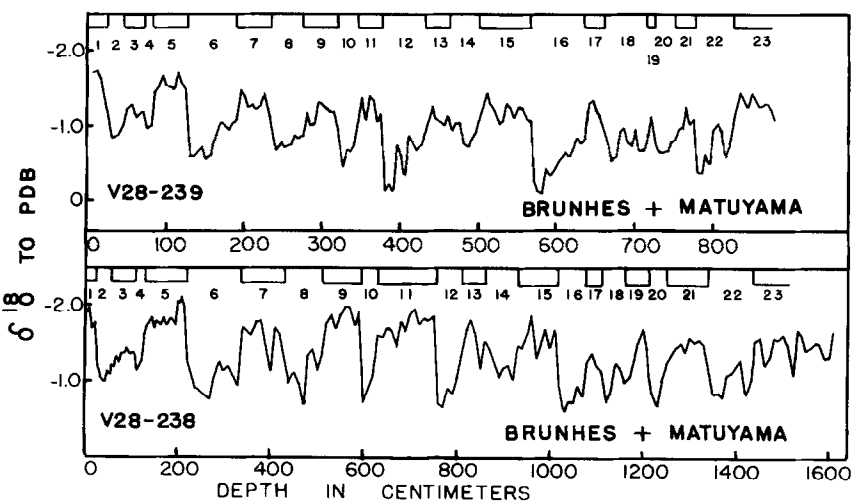

FIG. 1. Oxygen-isotope ratios for Western Pacific cores V28-238 and V28-239 containing the Brunhes–Matuyama magnetic reversal. Even (glacial) and odd (interglacial) stages are indicated above each isotope-ratio plot. Reproduced, with permission, from Shackleton and Opdyke (1976).

supportive comparisons with other long cores (e.g., Fig. 2). Thus major departures from uniformity are identified and only the more uniform sections are used for dating purposes.

VALIDITY OF THE METHOD OVER THE BRUNHES INTERVAL

Hays *et al.* (1976) have shown by frequency analysis that the dominant frequencies of Northern Hemisphere summer-insolation variations are found also in the $\delta^{18}O$ patterns of cores over the last 450,000 yr. The assumption is made in this paper that climate-coupling factors underlying the frequency-analysis results remained the same back to the Brunhes boundary. This assumption is probably satisfactory as suggested by $\delta^{18}O$ fluctuations of at least two-thirds of the late Pleistocene glacial amplitude that began 2.5 my ago (Shackleton and Opdyke, 1977). It is further supported by analyses of cores from the Central Arctic basin that indicate that Arctic Ocean ice cover has remained similar to present from the time of the onset of the Brunhes (Herman, 1974) from which it can be inferred that high-latitude climate conditions and fluctuations have remained much the same.

THE ASTRONOMICAL TIME SCALE AND INSOLATION VARIATIONS

The well-known work of Milankovitch (1930) was the first attempt to use planetary mechanics to calculate the zonal insolation variations during the latter Pleistocene from changes in the Earth's orbital parameters. Modern computing techniques and the precision to which the masses and orbital parameters of the planets are known have resulted in greatly improved calculations of the insolation variations for the last two million years. A comparison of the calculations of Vernekar (1972) with the later calculations of Berger (1978) which include more terms of the Jupiter–Saturn resonance suggests that the astronomical scale is now highly accurate over the last million years. Figure 3 compares insolation deviations from the present calculated by Vernekar with those calculated by Berger for the Northern Hemisphere summer half-year at two latitudes near 800,000 yr B.P. The dates of the insolation maxima given by each author do not differ by more than about 1000 yr. The uncertainty in the astronomical time scale compiled by Berger at this point of Pleistocene time is therefore probably not greater than about 1000 yr.

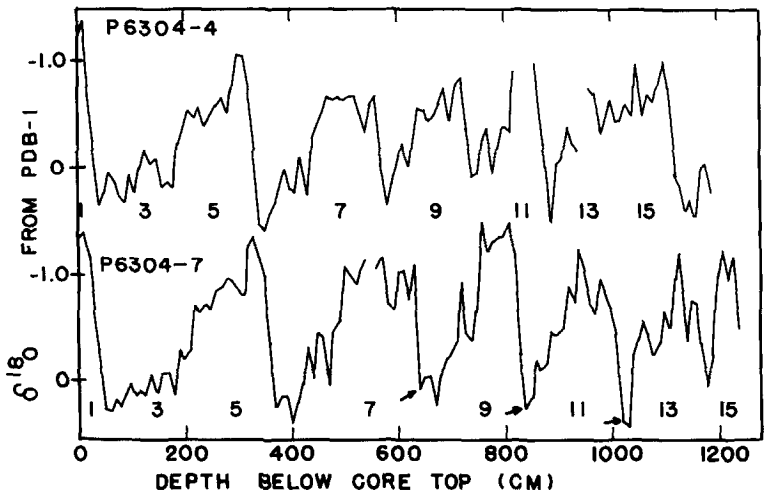

FIG. 2. Oxygen isotope ratios for cores P6304-4 and P6304-7 from the Caribbean. Odd numbers on each plot designate interglacial stages. Reproduced, with permission, from Emiliani (1972).

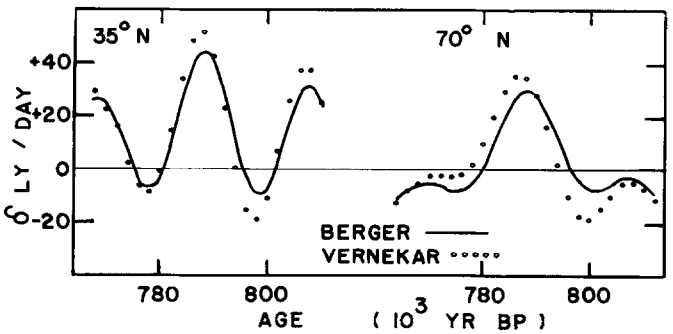

FIG. 3. Calculated Northern Hemisphere deviations from the present for summer half-year insolation averages of Berger (1976) (smooth curve), compared with Vernekar (1972) (closed circles), for latitudes 35°N and 70°N near 800,000 yr B.P.

In this paper summer-insolation deviations from 1950 values for two northern latitudes, 70°N and 35°N, are used to date the $\delta^{18}O$ features. The summer high-latitude insolation average is most strongly influenced by polar-axis inclination variations having a periodicity of about 40,000 yr. The low-latitude variation is largely dominated by the 22,000-yr precession effect which causes summers to occur periodically nearer to or farther from the sun. These insolation variations are strongly modulated by eccentricity variations with a periodicity of about 100,000 yr. The magnitude of change of the summer half-year insolation average between extremes of the precessional period occasionally approaches 10%, with a midsummer incident-radiation intensity change of as much as 20%.

INSOLATION AND ISOTOPE-RATIO FEATURE-IDENTIFICATION CONSIDERATIONS

The identification of tropical-core isotope-ratio features with their corresponding insolation variations rests on these assumptions: (1) The mass balance of Northern ice sheets is strongly influenced by long-term summer insolation changes in which the 22,000-yr precessional variation and the eccentricity variation are major factors. (2) The deepest minima in the isotope ratios occur at times of low eccentricity, usually near the end of such intervals, and in association with low summer insolation at all Northern Hemisphere latitudes. (3) The glacial-ice-volume variations are well represented by isotope-ratio changes in suitably uniform cores.

The first assumption is convincingly supported by the frequency analysis of summer insolation and core isotope ratios (Hays *et al.*, 1976). However, their results account for only part of the observed variance in the isotope ratios. Internal climate factors must also contribute to the variance. The application of the astronomical time scale must be done in the context of strong feedback factors that may favor long periods of ice-volume growth as well as the occasional major deglaciations suggested by the isotope-ratio record. The lagging changes in thermal inputs and heat transport due to the changing albedo of growing or shrinking ice sheets and altered oceanic and atmospheric circulation are comparable in magnitude in northern zones to orbitally induced insolation changes (Johnson and Andrews, 1979). Consequently the total effects of a specified insolation change on temperatures and precipitation will depend on the circulation patterns and ice-mass distribution at the time. In spite of these complexities, the frequency analysis clearly suggests the usefulness of the modulated precessional effect in the isotope ratio correlation process.

The second assumption, that deep isotope-ratio minima are associated with specific insolation minima, is suggested by the correlations in a uniform section of core

V28-238 (Fig. 4) and is consistent with physically plausible relations between Northern summer insolation and glacial mass balances. This association is the primary factor used in this paper to place the isotope-ratio features on the astronomical time scale over the lower part of the Brunhes. These close associations are plausible because, under conditions of established ice sheets and unfavorable atmospheric and oceanic circulation, it may be difficult for the weak summer insolation peaks resulting from low eccentricity to effectively remove Northern ice. Maximum total accumulation would then have followed at times of coinciding low insolation at 35°N and 70°N, perhaps with a short time lag. On the other hand, high insolation peaks at all latitudes caused by favorable precession and obliquity when the eccentricity is large did not always assure the removal of ice to the extent of the present interglacial extreme as can be seen by inspection of Figure 4. Such major deglaciations usually occurred only after major glacial extremes. A plausible speculation to explain this is that as summer insolation increased during the very early part of such deglaciations the deep southern penetration of the glacial front in eastern North America steered many subpolar storm systems first eastward over warm Gulf Stream water. Consequently unusually large masses of warm air would then have been transported northeastward into the high latitudes by these systems along the Atlantic polar water fronts that are depicted by Ruddiman and McIntyre (1973). This effect may have ensured the removal of most of the ice sheets during the subsequent interval of generally high summer insolation.

The third assumption, that ice volumes are reflected in the isotope ratios, is at times weakened by core-site factors; comparisons with other cores are necessary to develop correct feature identifications. Core-site factors may modify both the amplitude of the $\delta^{18}O$ variations and the net rate of deposition of sediment. Slight temperature changes of the foraminiferal habitat may influence the isotope-ratio amplitudes (Geitzenauer *et al.*, 1976). A more serious factor is the fluctuation of the carbonate dissolution rate in benthic water masses (Shackleton and Opdyke, 1976) that directly affects the net deposition rate.

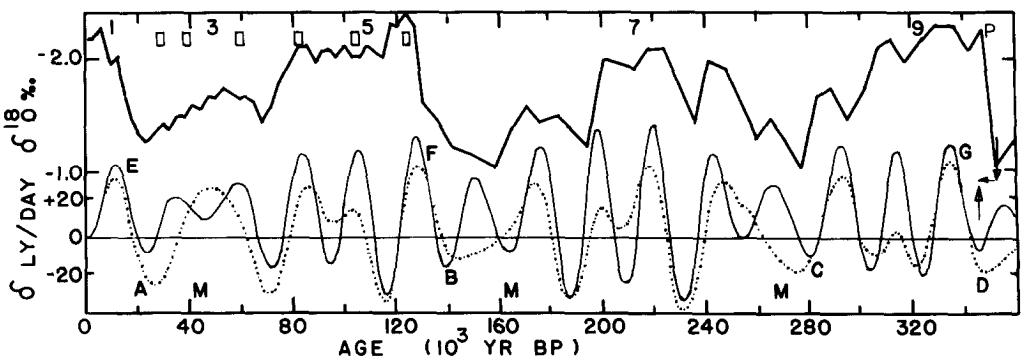

FIG. 4. Oxygen-isotope ratios (top broken line) for Stages 1 to 10 (top numbers) from core V28-238 compared with precession-dominated summer half-year insolation deviations for 35°N latitude (smooth curve), and inclination-dominated summer half-year insolation deviations for 70°N latitude (dotted curve). The age scale is the astronomical time scale. Insolation variations are given in average Langleys per day (cal cm^{-2} day^{-1}), deviation from year 1950. Small rectangles show dates of worldwide high sea stands (Bloom *et al.*, 1974). Repetitive responses of isotope ratios to insolation changes as cited in the text are indicated at A–G. Eccentricity minima are denoted by M. The high peak (P) may be anomalous as it is found in no other core. Offset opposed arrows in Stage 10 show lack of ideal coincidence of isotope-ratio minimum and insolation minima. Isotope ratios after Shackleton and Opdyke (1973). Insolation from the Berger tabulations, Berger, (1978).

Major erosional gaps or large changes in net deposition resulting from dissolution seem to have occurred at some points in all cores, and minor changes may occur between stadials and interstadials. Such effects can be adequately identified only by means of intercore comparisons. An effective method of comparison is a Shaw plot (Shaw, 1964) in which the isotope-ratio features common to two cores are plotted as a function of their downcore position on x and y axes, respectively. Abrupt slope changes in the plot reveal changes in net relative deposition rates and thus indicate the need for supportive information to ensure correct peak correlations. The Shaw plot simplifies the core analysis of this paper.

UNIFORMITY ANALYSIS OF V28-238 AND V28-239

The oxygen-isotope ratios for these cores are those of *Globigerina sacculifera*, a planktonic species. The cores are located about 290 km apart on northern flanks of the Ontong-Java Plateau, a region that is not subject to sedimentation changes caused by water- or airborne particulates from land. The sea-surface temperature variation here is minimal. However some locations on the plateau flanks are subject to occasional erosion by currents or by sliding as shown in acoustic profiles (Berger and Johnson, 1976). Probably a more generally significant factor is the influence of dissolution on the net deposition rate. Dissolution has removed a substantial part of the sediment at the core depths as shown by reduced sediment thicknesses in the acoustic profiles. Dissolution rate changes can alter both the deposition rates and the isotope ratios (Erez, 1979). An increase in the rate, for example, will slow the net deposition rate and move the measured oxygen-isotope ratio toward lower (more positive) values because dissolution selectively removes the smaller individual forams that lived closer to the surface in warmer water layers (Savin and Douglas, 1973).

These effects can explain the major nonuniformities in the Shaw plot of Figure 5. Corresponding isotope-ratio features in each core, mostly precessional maxima or minima, are plotted as a function of downcore position on the two coordinate axes. Distinct changes in relative deposition rates are indicated at A–D. The points between A and B depart very little from a fitted straight line, which, however, does

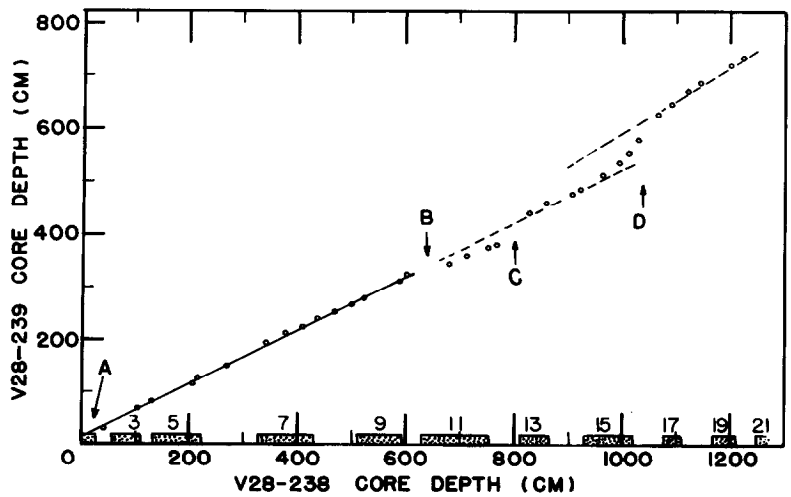

FIG. 5. A Shaw plot for selected isotope-ratio features common to cores V28-238 and V28-239. Interglacial stages in V28-238 are indicated by odd numbers. Departures from uniform deposition in one of the cores are indicated at A–D.

not intersect the zero point. This departure from zero is associated with V28-239 in which a rise in the interglacial-stage peaks toward the present suggests progressively reduced dissolution. The rise is climaxed by anomalously thick strata in Stage 1 relative to other cores (Figs. 1 and 2). Therefore the more uniform section of V28-238 from Stage 1 to 10 is selected for further analysis.

At B a departure from the fitted line indicates a discontinuity, and there are fewer peaks in Stage 11 in V28-239 than in V28-238 (Fig. 1). Unpublished data indicate that the Stage 11 section in V28-238 was stretched during core recovery (N. G. Pisias, pers. commun., 1980). To assess the magnitude of this effect, the extended lengths of Stage 11 and Stage 9 were compared in seven additional cores in which the stage features were clearly identifiable. The length of each stage was best defined by the distance between the last low isotope-ratio points preceding the sharp glacial terminations (indicated typically by the small arrows in Fig. 2). The ratios of stage lengths are shown in Table 1. The average ratio of 0.91 for the seven cores when compared with a ratio of 1.00 for V28-238 suggests that Stage 11 may be stretched by about 10%. In V28-239 the ratio is only 0.65, suggesting a substantial sediment loss in Stage 11 of that core. For further analysis the selected core section between Stages 10 and 12 is therefore that of V28-238 uniformly reduced in length by 9%.

The discontinuity at C in Stage 12 is apparently caused by sediment loss in V28-238. The relatively thicker strata found in V28-239 (Fig. 1) between the high isotope-ratio peak of Stage 13 and the Stage 12 minimum is consistent with corresponding thicker strata in the cores of Figure 2. The selected section for Stages 12 to 14 is therefore that of V28-239. The steeper slope defined by the points at D (Fig. 5) indicates a broad change in relative deposition rates between the two cores. The effect begins near the Brunhes boundary, Stage 19, reaches a climax in the upper part of Stage 16, and returns to normal in Stage 14. The steeper slope may be explained by a greater sediment loss resulting, at least in part, from a more rapid dissolution rate in V28-238 as suggested by the relatively low major peak of Stage 17 and the smaller number of peaks visible in Stages 16–18 (Fig. 1). The selected sections in this interval are therefore those of V28-239.

The selection of the most uniform core sections to match insolation with $\delta^{18}O$ variations is the key to the establishment of the isotope-ratio time scale from the present to the Brunhes boundary. The matching and the determination of sediment deposition

TABLE 1. CORES USED IN THE STUDY

Core	Location	Depth (m)	Ratio	Reference
P6408-9	15°N–69°W	4098	0.79	Emiliani (1978)
P6304-7	15°N–69°W	3929	0.90	Emiliani (1972)
P6304-4	15°N–71°W	4136	0.94	Emiliani (1972)
P6304-8	15°N–69°W	3928	0.82	Emiliani (1966)
P6304-9	15°N–69°W	4126	0.95	Emiliani (1966)
RC14-37	1°N–90°E	2226	0.90	Shackleton (1977)
E49-18	46°S–90°E	3256	1.09	Hays *et al.* (1976)
Average Stage 11/Stage 9 ratio: 0.91 ± 0.09				
V28-238	1°N–160°E	3120	1.00	Shackleton and Opdyke (1973)
V28-239	3°N–159°E	3490	0.65	Shackleton and Opdyke (1976)

Note. The ratio of extended core lengths (Stage 11/Stage 9) in the first seven cores is used to assess the probable amount of stretching of Stage 11 in V28-238.

rates used in the analyses are described in detail in the following two sections. The guiding criteria for the analyses can be summarized as follows: In Stages 1 to 10 of the uniform section of core V28-238 (Fig. 4), each major $\delta^{18}O$ minimum falling in the lowest 25% of the $\delta^{18}O$ range is assumed to have occurred at the astronomical time-scale position of the nearest pair of low- and high-latitude insolation minima. Probable time lags are neglected. Except for a minor adjustment of the glacial Stage 10 $\delta^{18}O$ minimum, little or no relocation of these minima on the astronomical time scale is required. In Stages 10–20 of the less uniform sections of the cores (Figs. 6–10), each of the interglacial core sections identified by Shackleton and Opdyke (1976) is considered sequentially. Each deepest glacial stage $\delta^{18}O$ minimum before and after the interglacial is likewise assumed to have occurred at the astronomical time-scale position of the nearest pair of low- and high-latitude insolation minima. After determining the match, and before proceeding to the next-older section, the length of the section is uniformly expanded or contracted by a minor amount if necessary to fit each deepest isotope minimum to the time-scale position of the corresponding insolation minima. Having established the time-scale positions of all major $\delta^{18}O$ minima, the identification of major $\delta^{18}O$ peaks with nearest pairs of insolation maxima (Figs. 6–10) is straightforward.

UPPER CORE-SECTION ANALYSIS

In Figure 4 the oxygen-isotope ratios from the upper 600 cm of core V28-238 (broken line) are compared with 35°N and 70°N latitude summer-insolation deviations. The time scale for the $\delta^{18}O$ curve was set by assuming an age of 124,000 yr B.P. for the interglacial high point at a 210-cm depth in the core to yield a uniform sedimentation rate of 1.694 cm/10^3 yr. This age is in agreement with the thorium–uranium age of 124,000 ± 5000 yr B.P. of coral reefs given by Broecker *et al.* (1968) for the Stage 5e high-sea stand on Barbados, and the age of 125,000 ± 4000 yr B.P. given by Harmon *et al.* (1981) for the 5e stand on Bermuda. This sedimentation rate provides a match of the low-latitude precession-dominated insolation peaks to the principal $\delta^{18}O$ peaks and to the dated high sea levels younger than the last interglacial (Bloom *et al.*, 1974). The variable phase relations between the two types of peaks may result in part from minor brief variations in net deposition rate.

The close association of the isotope-ratio minima of glacial extremes with times of low insolation at all latitudes during low eccentricity intervals M is evident in Figure 4 at A–D. Only when such extremes were followed immediately by coincident high- and low-latitude peaks E–G did deglaciation to the present isotope-ratio level occur. It is noteworthy that weak precessional insolation peaks that are accompanied by no high-latitude insolation excess (near A–D, Fig. 4) result in little or no isotope-ratio response.

LOWER CORE-SECTION ANALYSES

Identification of isotope-ratio features beyond 340,000 yr B.P. begins with glacial Stages 10 to 12 (Fig. 6). The Stage 10 glacial extreme is set coincident with the insolation minimum (opposed arrows) prior to the 335,000-yr B.P. synchronized insolation peaks, and the isotope ratios of V28-238 are plotted back to Stage 12 using the section length reduced by 9% (as discussed earlier) and the deposition rate of 1.694 cm/10^3 yr established for the upper 600 cm of the core. The Stage 12 isotope-ratio extreme is clearly associated with the synchronized insolation minima of 436,000 yr B.P., the opposed arrows slightly offset on the right suggesting a slight departure from an optimum match of minima. Principal isotope-ratio peaks at A and B correspond to the two pairs of high- and low-latitude coincident insolation peaks. This procedure is repeated sequentially as follows for the lower core sections from V28-239 for which an

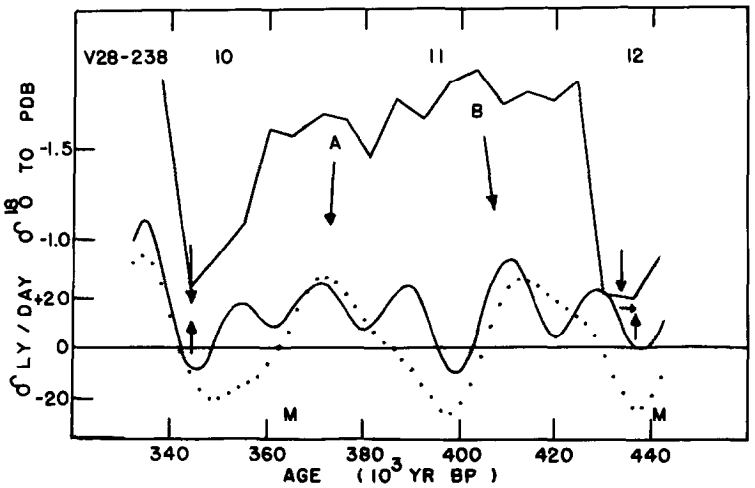

FIG. 6. Isotope ratios for Stages 10 to 12 in core V28-238 compared with insolation deviations from year 1950. Opposed arrows in Stage 10 show the reset isotope-ratio minimum in coincidence with insolation minima. Offset opposed arrows in Stage 12 indicate lack of ideal coincidence of isotope and insolation minima. Isotope-ratio peaks corresponding to high- and low-latitude coincident maxima are indicated at A and B. Solid lower curve refers to 35°N latitude insolation; dotted curve, to 70°N latitude insolation. Eccentricity minima are denoted by M.

average upper core-section deposition rate of 0.920 cm/10^3 yr is used.

In Stages 12 to 14 (Fig. 7), the five isotope-ratio peaks rise and fall with the envelope of the low-latitude insolation peaks in a manner similar to the peak envelopes of Figure 4. In Stages 14 to 16 (Fig. 8), the principal precessional peaks A–C are again easily identified with their isotope-ratio counterparts. In Figure 9 the designated best Stage 18 insolation low-point match places the isotope-ratio peak A coincident with the most favorable all-latitude insolation peak. Other isotope-ratio peaks are not clearly identifiable, although the isotope-ratio profile resembles the precessional insolation envelope as usual. In Stages 18 to 20 (Fig. 10), the prom-

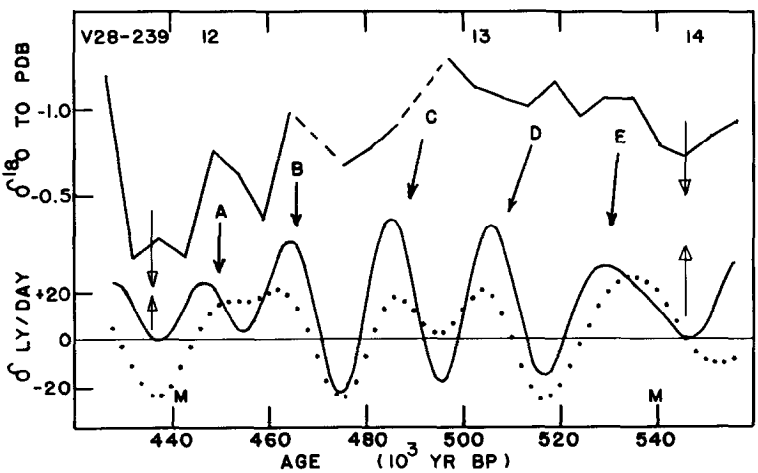

FIG. 7. Isotope ratios for Stages 12 to 14 in core V28-239 compared with insolation deviations. Legend as in Figure 6.

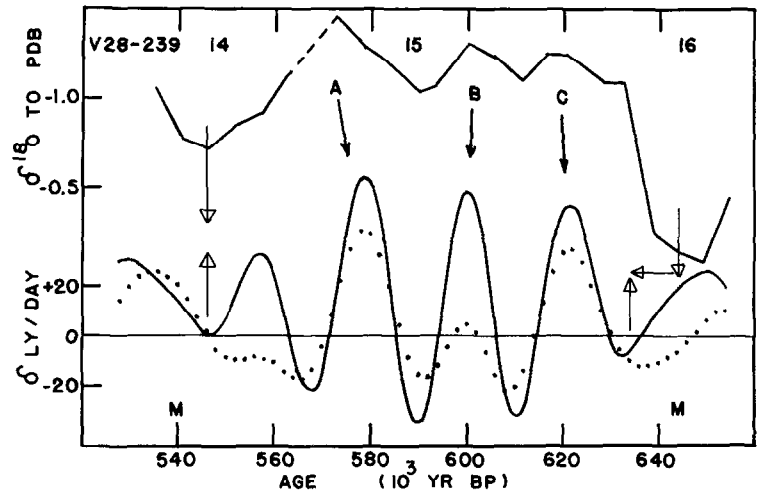

FIG. 8. Isotope ratios for Stages 14 to 16 in core V28-239 compared with insolation deviations. Legend as in Figure 6.

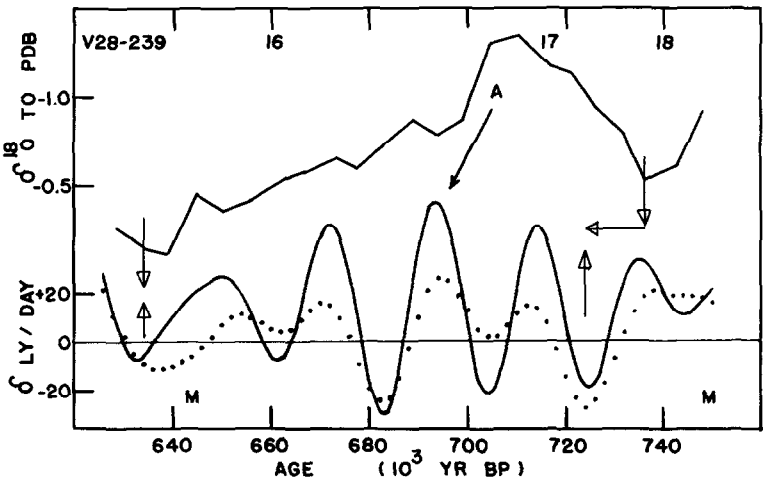

FIG. 9. Isotope ratios for Stages 16 to 18 in core V28-239 compared with insolation deviations. Legend as in Figure 6.

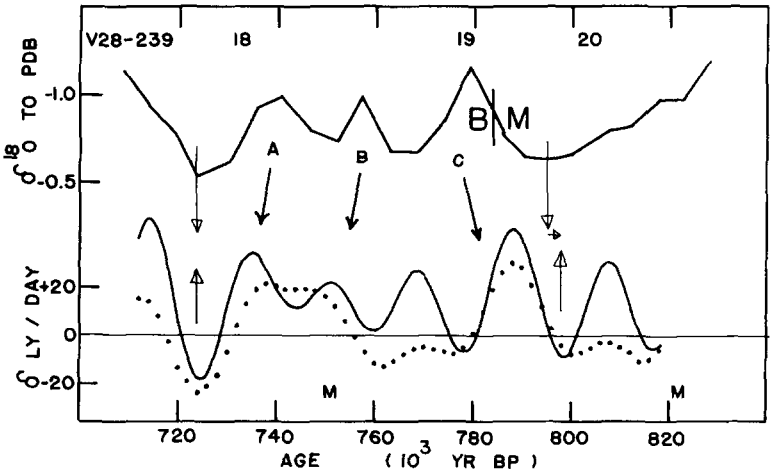

FIG. 10. Isotope ratios for Stages 18 to 20 in core V28-239 compared with insolation deviations. Legend as in Figure 6. The Brunhes–Matuyama boundary is shown here at 724 cm on the isotope-ratio curve with a most probable time-scale position near the top of the high- and low-latitude coincident insolation maxima at 788,000 yr B.P.

TABLE 2. RESIDUALS ($S - A$) BETWEEN SEDIMENTARY TIME INTERVALS AND CORRESPONDING ASTRONOMICAL TIME-SCALE INTERVALS BETWEEN KEY INSOLATION MINIMA[a]

Core	Stage interval	Section length (cm)	Sedimentary interval, S (10^3 yr)	Astronomical interval, A (10^3 yr)	$S - A$ (10^3 yr)
V28-238	1–10	600	354	344	10
V28-238	10–12	150[b]	89	92	−3
V28-239	12–14	101	110	110	0
V28-239	14–16	90	98	88	10
V28-239	16–18	94	102	90	12
V28-239	18–20	66	72	74	− 2

[a] The stage intervals are from the present to the $\delta^{18}O$ minimum of Stage 10, and between $\delta^{18}O$ minima thereafter. The sedimentation rate of 1.694 cm/10^3 yr for V28-238 is chosen consistent with the Stage 5e radioisotope date and with an optimum match of $\delta^{18}O$ peaks to precessionally dominated insolation peaks in Stages 1–10. This rate is used to calculate the age of the Stage 9 point at 580 cm in V28-238 from which the sedimentation rate of 0.920 cm/10^3 yr is calculated for the corresponding point at 315 cm in V28-239. These rates are then used to estimate the remaining sedimentary time intervals (S).

[b] This length is reduced by 9% from the original section length as described in the text.

inent isotope-ratio peak C containing the Brunhes–Matuyama reversal is a response to the only nearby pair of coincident insolation peaks centered at 788,000 yr B.P. Table 2 summarizes the age residuals resulting from the sequential fitting of the isotope-ratio data to the astronomical time scale.

DISCUSSION

The Brunhes–Matuyama reversal occurs in Stage 19 at the 724-cm downcore position in core V28-239 (Opdyke, 1980), about 4000 yr below the isotope-ratio maximum of a strong precessional peak (Fig. 10). In V28-238 it occurs at 1200 cm in an equivalent position on a slightly asymmetrical peak (Fig. 1). The isotope-ratio peak probably lagged the insolation peaks at 788,000 yr B.P. somewhat. The Holocene deglaciation, for example, lagged the 10,000-yr B.P. insolation peak by about 5000 yr (Bryson *et al.*, 1969). Therefore the reversal is likely to have occurred very close to the insolation maxima, and the most probable age for the reversal is 790,000 yr B.P. with a probable uncertainty of less than 5000 yr.[1]

The new isotope-ratio time scale derived by the method of this paper is compared in Figure 11 with recent time scales derived by Emiliani (1978) and by Kominz *et al.* (1979). The new scale is in close agreement with the Emiliani scale to Stage 14, and with the Kominz scale to Stage 16. The older location of the Brunhes boundary at 790,000 yr B.P. on the new scale depends largely on the assumption that Stages 12 to 13 and Stages 16 to 19 in V28-239 have a better approximation to the upper-core deposition rate than do the same stages in V28-238. This is supported by relative section lengths in other cores and by the argument of excessive dissolution in V28-238. On the other hand the use of these stages from V28-238 would result in glacial extremes near eccentricity maxima and a gross failure of the

[1] This is the age of the stratum in which the reversal is found in core V28-239. However, remagnetization of less-consolidated sediments at the surface of the two core locations may have occurred at the time of the reversal event, thus displacing the observed reversal to older, different, downcore positions on the isotope-ratio profiles. Close examination of the data from both cores indicates that, relative to the Stage 19 isotope-ratio peak, the reversal in V28-239 is about 3 cm below the position in that core that is suggested by the reversal in V28-238. Assuming that the remagnetized layer is the same thickness in each core, and using the average deposition rates of this paper, the age of the reversal event is found to be 7000 yr younger than the 790,000-yr age of the reversal stratum in V28-239. The remagnetization possibility was suggested by Charles Barton.

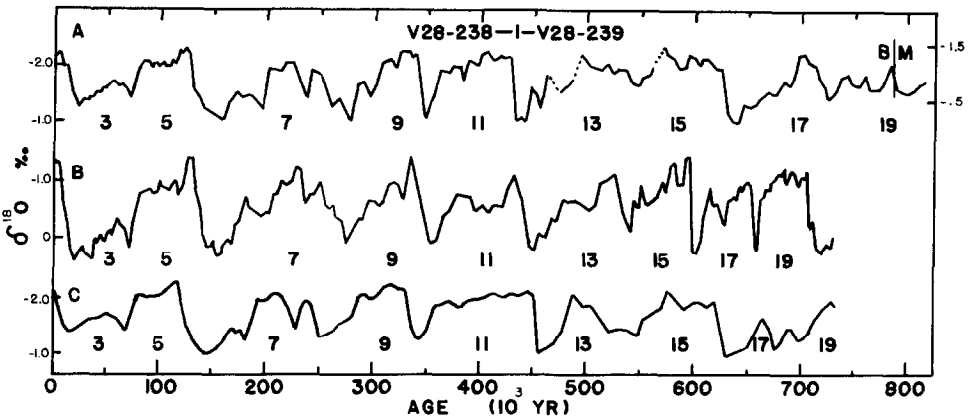

FIG. 11. Comparison of the new isotope-ratio time scale A with the time scales of Emiliani (1978) B and Kominz *et al.* (1979) C.

peak-envelope match, and so would be inconsistent with the criteria established from the uniform section of V28-238. Thus consistency with other cores and within the two principal cores of the study supports the use of these critical sections from V28-239.

CONCLUSION

The occurrence of gaps in core strata and the lack of large time-scale uniformity of sediment deposition is a serious obstacle to $\delta^{18}O$ dating efforts over the Brunhes interval. The duplication of the principal isotope-ratio glacial-stage features over this interval in two well-separated tropical cores, V28-238 and V28-239, suggests that these cores are of superior uniformity, although a problem of variable deposition is clearly present. The method of this paper addresses this problem (1) by core analysis using the Shaw plot technique and intercore comparisons, (2) by assuming small-scale uniformity in selected core sections between glacial extremes, and (3) by sequentially matching extreme minima in the isotope ratios to the astronomical time scale at points of generally low summer insolation during times of low orbital eccentricity. This fitting process is accomplished easily and yields age residuals that are substantially smaller than those of any alternative matches. The process also yields a satisfactory correspondence between the envelope of principal isotope-ratio peaks and the envelope of precessional insolation peaks. This correspondence strongly supports the resulting age of 790,000 yr B.P. for the Brunhes boundary.

ACKNOWLEDGMENTS

A. L. Berger kindly supplied the tabulated results of his insolation calculations. N. D. Opdyke provided additional precision for the position of the Brunhes boundary in core V28-239. The reviewers provided many valuable suggestions.

REFERENCES

Berger, A. L. (1978). Long-term variations of caloric insolation resulting from the Earth's orbital elements. *Quaternary Research* 9, 139–167.

Berger, W. H., and Johnson, T. C. (1976). Deep-sea carbonates: Dissolution and mass wasting on the Ontong-Java Plateau. *Science* 192, 785–787.

Bloom, A. L., Broecker, W. S., Chappell, J. M. A., Matthews, R. K., and Mesolella, K. J. (1974). Quaternary sea level fluctuations on a tectonic coast: New $^{230}Th/^{234}U$ dates from the Huon Peninsula, New Guinea. *Quaternary Research* 4, 185–205.

Broecker, W. S., Thurber, D. L., Goddard, J., Ku, T., Matthews, R. K., and Mesolella, K. J. (1968). Milankovitch Hypothesis supported by precise dating of coral reefs and deep sea sediments. *Science* 159, 297–300.

Bryson, R. A., Wendland, W. M., Ives, J. D., and Andrews, J. T. (1969). Radiocarbon isochrones on the disintegration of the Laurentide ice sheet. *Arctic and Alpine Research* 1, 1–14.

Cox, A., and Dalrymple, G. B. (1967). Statistical

analysis of geomagnetic reversal data and the precision of potassium–argon dating. *Journal of Geophysical Research* **72**, 2603–2614.

Dansgaard, W., and Tauber, H. (1969). Glacier oxygen-18 content and Pleistocene ocean temperatures. *Science* **166**, 499–502.

Emiliani, C. (1955). Pleistocene temperatures. *Journal of Geology* **63**, 538–578.

Emiliani, C. (1972). Quaternary paleotemperatures and the duration of the high temperature intervals. *Science* **178**, 398–401.

Emiliani, C. (1978). The cause of the Ice Ages. *Earth and Planetary Science Letters* **37**, 349–352.

Erez, J. (1979). Modification of the oxygen-isotope record in deep-sea cores by Pleistocene dissolution cycles. *Nature (London)* **281**, 535–538.

Geitzenauer, K. R., Roche, M. B., and McIntyre, A. (1976). Modern Pacific coccolith assemblages: Derivation and application to late Pleistocene paleotemperature analysis. *In* "Investigation of Late Quaternary Paleoceanography and Paleoclimatology" (R. R. Cline and J. D. Hays, Eds.). *Geological Society of America Memoir* **145**, 423–449.

Harmon, R. S., Land, L. S., Mitterer, R. M., Garrett, P., Schwarcz, H. P., and Larson, G. J. (1981). Bermuda sea level during the last interglacial. *Nature (London)* **289**, 481–483.

Hays, J. D., Imbrie, J., and Shackleton, N. J. (1976). Variations in the Earth's orbit: Pacemaker of the Ice Ages. *Science* **194**, 1121–1132.

Herman, Y. (1974). Arctic Ocean sediments, Microfauna, and the climatic record of Late Cenozoic time. *In* "Marine Geology and Oceanography of the Arctic Seas" (Y. Herman, Ed.), p. 288. Springer-Verlag, New York.

Johnson, R. G., and Andrews, J. T. (1979). Rapid ice-sheet growth and initiation of the last glaciation. *Quaternary Research* **12**, 119–134.

Kominz, M. A., Heath, G. R., Ku, T. L., and Pisias, N. G. (1979). Brunhes time scales and the interpretation of climatic change. *Earth and Planetary Science Letters* **45**, 394–410.

Mankinen, E. A., and Dalrymple, G. B. (1979). Revised geomagnetic polarity time scale for the interval 0–5 m.y. BP. *Journal of Geophysical Research* **84**, 615–626.

Milankovitch, M. (1930). Mathematische Klimalehre und astronomische theorie der klimaschwankungen. *In* "Handbuch der Klimatologie I" (T. A. Gebruder, Ed.). Borntraeger, Berlin.

Opdyke, N. D. (1980). Personal communication.

Ruddiman, W. F., and McIntyre, A. (1973). Time-transgressive deglacial retreat of polar waters from the North Atlantic. *Quaternary Research* **3**, 117–130.

Savin, S. M., and Douglas, R. G. (1973). Stable isotope and magnesium geochemistry of recent planktonic foraminifera from the South Pacific. *Geological Society of America Bulletin* **84**, 2327–2342.

Shackleton, N. J. (1977). The oxygen isotope stratigraphic record of the Late Pleistocene. *Philosophical Transactions of the Royal Society of London B* **280**, 169–182.

Shackleton, N. J., and Opdyke, N. D. (1973). Oxygen isotope and paleomagnetic stratigraphy of equatorial Pacific core V28-238: Oxygen isotope temperatures and ice volumes on a 10^5 and 10^6 year scale. *Quaternary Research* **3**, 39–55.

Shackleton, N. J., and Opdyke, N. D. (1976). Oxygen-isotope and paleomagnetic stratigraphy of Pacific core V28-239 Late Pliocene to Latest Pleistocene. *In* "Investigation of Late Quaternary Paleoceanography and Paleoclimatology" (R. R. Cline and J. D. Hays, Eds.). *Geological Society of America Memoir* **145**, 449–464.

Shackleton, N. J., and Opdyke, N. D. (1977). Oxygen isotope and paleomagnetic evidence for early Northern Hemisphere glaciation. *Nature (London)* **270**, 216–219.

Shaw, A. B. (1964). "Time in Stratigraphy." McGraw–Hill, New York.

Vernekar, S. D. (1972). "Long-Period Global Variations of Incoming Solar Radiation." Meteorological Monographs 8, No. 30. Amer. Meteorol. Soc., Boston.